Available online at www.sciencedirect.com

ScienceDirect

Procedia Manufacturing 48 (2020) 379–387

Procedia MANUFACTURING

www.elsevier.com/locate/procedia

48th SME North American Manufacturing Research Conference, NAMRC 48 (Cancelled due to COVID-19)

A feasibility study of continuous grain refinement of sheet metal

T. Ha[a,b], R. Murudkar[c], K. T. Hartwig[c], T. Welo[b], G. Ringen[b], and J. Wang[c,d,*]

[a]*Interdisciplinary Engineering, College of Engineering, Texas A&M University, College Station, Texas 77843, USA*
[b]*Department of Mechanical and Industrial Engineering, Norwegian University of Science and Technology, Trondheim 7491, Norway*
[c]*Department of Mechanical Engineering, Texas A&M University, College Station, Texas 77843, USA*
[d]*Department of Engineering Technology and Industrial Distribution, Texas A&M University, College Station, Texas 77843, USA*

* Corresponding author. Tel.: +1-979-845-4903 ; fax: +1-979-862-7969. *E-mail address:* jwang@tamu.edu

Abstract

Various severe plastic deformation (SPD) techniques have been used to develop ultrafine-grained (UFG) materials to enhance material properties. Equal channel angular extrusion/pressing (ECAE/ECAP) is an effective technique to severely deform material and refine grains, however, the drawback is that a continuous process on sheet metal is confined due to the process mechanism. Equal channel angular drawing (ECAD), a continuous strip drawing process, has limitations in achieving grain refinement because drawing is a stretching phenomenon contrary to an extrusion or pressing process. In the present work, experiments were conducted on interstitial-free (IF) steel to demonstrate that grain refinement of thin sheets can be achieved through pack extrusion; and while there was shear deformation, ECAD failed to produce UFG microstructure. The finite element analysis showed the sheet metals have distinctive stress-strain states after ECAE and ECAD. The feasibility of combining ECAE and ECAD to approach the stress-strain state of the sheet metal in pack extrusion for grain refinement was investigated. Simulation results showed that with proper loading conditions, continuous grain refinement of thin metal strips is sufficiently possible.

Keywords: Severe plastic deformation; ECAE; ECAD; Continuous process; Grain refinement; Sheet metal

1. Introduction

Severe plastic deformation (SPD) processes have been used to obtain ultrafine-grained (UFG) materials for improving strength, hardness, and material properties by material processing techniques such as equal channel angular extrusion/pressing (ECAE/ECAP), equal channel angular drawing (ECAD), accumulative roll bonding (ARB), repetitive corrugation and straightening, and con-shearing. Conventional metal forming processes such as rolling, drawing, or pressing may also lead to grain refinement for the materials. However, those are not efficient methods to develop ultra-fine grain compared to the SPD process.

ECAE, developed by Segal [1–4], is a working process to refine grains by using two different direction channel dies having an equal circular or square cross-section in the initial and final process. The material is pressed through the die inlet and deformed severely passing through the die corner as shown in Fig. 1 where φ is the channel intersection angle and ψ is the curvature angle at the intersection point in the two channels. These two angles are dominant parameters to formulate the strain relations by Segal [1] and Iwahashi et al. [5].

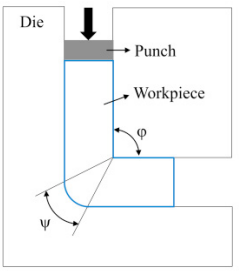

Fig. 1. Equal channel angular extrusion/pressing

The material properties or grain refinement can be improved by repeating the process and increasing the severe deformation

2351-9789
10.1016/j.promfg.2020.05.060

of the workpiece [6]. The routes and repetitive pressings determine microstructure shear patterns and grain sizes. The fundamental routes are route A, B_A, B_C, and C as shown in Fig. 2. These four different routes make various microstructure shear patterns due to the constant shape of the die corner. For example, the shear plane angle is 45° in perpendicularly crossing channels. The workpiece or billet in route A has the same passing direction without rotating the workpiece. The repeated process of route A results in a lamellar-type microstructure. The workpiece rotates ±90° for two passes of route B_A and 90° for each pass of route B_C. The route B_A results in distorted microstructures. Route C has the same shear plane because the workpiece rotates 180° each extrusion, but it has the opposite shear direction. For high purity aluminum, route B has fast grain evolution compared to route A and C, where there is a 0° and 180° rotation after each pass, respectively [7]. While routes B_A, B_C, and C are used to achieve grain refinement of a billet, the rotating process of the workpiece makes the process discontinuous. Thus, only route A was considered to expand an ECAE process into a continuous process.

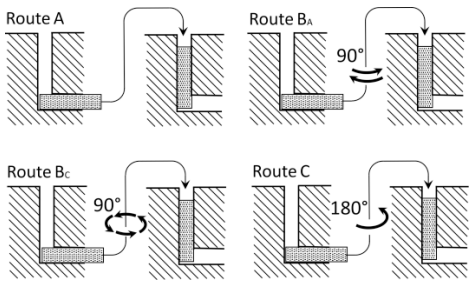

Fig. 2. The fundamental routes in ECAE process procedure [6]

Shear strain, γ, and effective strain, ε, for ECAE were presented by assuming material deformation to be simple shear in the following Eqs. (1) and (2) by Segal [1] and Eqs. (3) and (4) by Iwahashi et al. [5]:

$$\varepsilon_N = \frac{N}{\sqrt{3}}\left[2\cot\left(\frac{\varphi}{2}\right)\right] \tag{1}$$

$$\gamma = 2\cot\left(\frac{\varphi}{2}\right) \tag{2}$$

$$\varepsilon_N = \frac{N}{\sqrt{3}}\left[2\cot\left(\frac{\varphi}{2}+\frac{\psi}{2}\right)+\psi\csc\left(\frac{\varphi}{2}+\frac{\psi}{2}\right)\right] \tag{3}$$

$$\gamma = \left[2\cot\left(\frac{\varphi}{2}+\frac{\psi}{2}\right)+\psi\csc\left(\frac{\varphi}{2}+\frac{\psi}{2}\right)\right] \tag{4}$$

According to Eq. (1), the total strain is determined by the number of passes, N, and the channel intersection angle, φ. The curvature angle, ψ, was not considered. Accordingly, the strain for one pass and 90° channel angle turns into 1.1547. The friction effect between material and die was not considered in Segal's and Iwahashi's strain relations. This may cause slightly different results compared to the real process result. However, the result from ECAE simulation with low friction coefficient has good agreement with the experiment results of polymers, high density polyethylene and polypropylene [8].

In the late '90s, ECAD [9,10] was applied to develop microstructures using 99.9 % pure aluminum. The noticeable strength development was obtained from each ECAD process with three routes, 0° rotation, reversed drawing direction, and 90° rotation, respectively. However, the severe plastic deformation by ECAD was not significant beyond two or multiple passes due to the thickness reduction and material elongation during the process [9,11,12]. The ECAD process using an AA1370 wire was used to recrystallize a microstructure; the drawing stress was more dominant than the shear stress and the workpiece diameter was reduced [13]. Weak shear deformation from ECAD is not efficient to achieve ultra-fine grain, but there is feasibility to apply for the continuous process on account of the pulling mechanism as shown in Fig. 3, nonetheless.

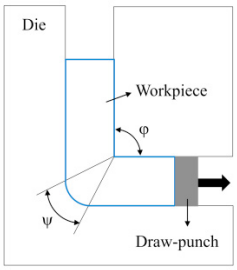

Fig. 3. Equal channel angular drawing

Micron or nano-sized grains in various metal materials can be formed by SPD process techniques with equal cross-section [14], however, those techniques have the limitation in the application of a continuous process and equiaxed grain formation. The continuous equal channel angular process by Chaudhury et al. [15] was invented and introduced for billets by adopting a roller system or a conveyor system for pushing and drawing of materials. Recently, a continuous four-pass adopted process was investigated for developing material properties of steel A580 GR36 alloy wire, and the pressing-drawing process is shown as a potent technique to gain ultra-fine grain refinement [16]. Therefore, the continuous SPD processing may work because structural instability like buckling can be almost removed in the feeding region.

In this paper, the potential of a continuous process for sheet metal was investigated by combining ECAE and ECAD into a single process. The effects of each open channel drawing and ECAE process on the material behavior were explored, and the microstructures were observed after each processing. The stress and strain states resulted from the simulations of different loading conditions were analyzed to predict the effectiveness of the combined ECAE/ECAD process.

2. Experiments

2.1. Open channel drawing and pack ECAE processes

Firstly, the interstitial-free (IF) steel workpiece was prepared in the dimension of 44 mm × 200 mm with 0.7 mm thick for the open channel drawing. The interface between the sheet metal and die was lubricated with light oil to reduce the effect of friction. Then, the IF steel sheet was pulled with an approximate speed of 12.7 mm/s at room temperature with a draw-bench.

The drawing system as shown in Fig. 4 was designed to simply pull the IF steel sheet and measure the drawing force during the process. A fish scale was connected to the rigid bars to measure the drawing force. The stroke length and drawing force at particular time steps were obtained.

Fig. 4. Open channel drawing assembly

Secondly, twelve IF steel sheets for pack ECAE were pressed into an IF steel can slot, and each end of the IF steel can was locked using plugs of IF steel (see Fig. 5). The dimension of the packed sheets was 8 mm × 16 mm × 200 mm and the approximate extrusion speed was 2.5 mm/s. A heavy grease lubricant was also applied to the contact regions between the billet and channel wall before pressing to reduce the effect of friction.

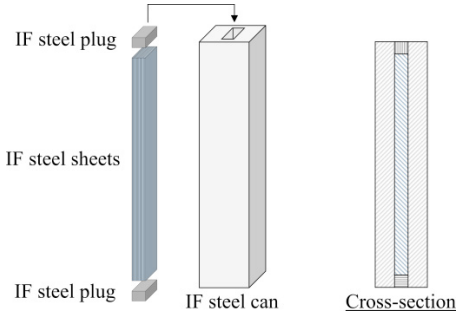

Fig. 5. Schematic of ECAE workpiece assembly

2.2. Optical microscopy

Microstructure evolution of IF steel sheets were observed for both the open channel drawing and ECAE processes with a Nikon Epiphot metallograph. The specimens were sectioned with an abrasive wheel, ground, and polished to eliminate contamination and impure surface. Fig. 6 shows the microstructure of the as-received IF steel sheet. The uniformly formed grain is observed in the flow plane while the grains show slight elongation in the transverse plane.

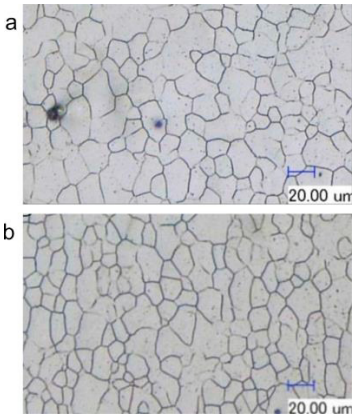

Fig. 6. As-received samples across the thickness (a) along the flow plane; (b) along the transverse plane

The microstructure at the bottom edge was slightly refined after the drawing process as shown in Fig. 7. The die contact region was at the bottom edge and the die radius affected the grain refinement. Also, heating effect was observed in Fig. 7(b) due to contact friction with the die.

The microstructure after route 1A of pack ECAE, shown in Fig. 8, was highly refined compared to the as-received grain structure shown in Fig. 6. The elongated and refined grains were observed. While the drawing process caused the microstructure to be locally refined at the contacting region with the drawing die, the pack ECAE process refined the overall microstructure of the sheet metal. The experiments showed that ECAE is a very effective technique to refine microstructure without changing the cross-section area. The grain distribution was not homogeneous by passing a route 1A of ECAE. However, UFG could be obtained with repetitive ECAE processes.

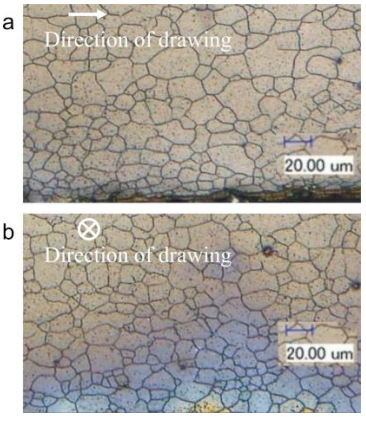

Fig. 7. Optical micrograph after the drawing process (a) along the flow plane; (b) along the transverse plane

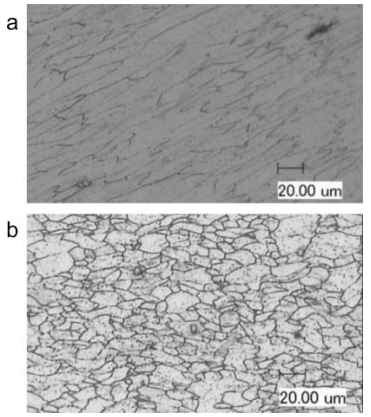

Fig. 8. Optical micrograph after ECAE route 1A (a) on the flow plane; (b) on the longitudinal plane

3. Finite Element Simulation based on Experiments

Since ECAD and pack ECAE created different microstructure from the experiments, finite element (FE) process simulations were conducted to investigate the stress-strain state of the material after ECAD and ECAE. Indeed, the FE analysis/simulation showed the stress-strain resulted from the two processes were different.

The plane stress for ECAD, Fig. 9(a), and the plane strain for the ECAE, Fig. 9(b), were simulated to understand the plastic deformation behavior of IF steel by the commercial code ABAQUS/Explicit. The material properties of IF steel were shown in Table 1. The meshes for work-pieces were modeled by employing 4-node bilinear quadratic elements, CPS4R for open channel drawing and CPE4R for ECAE. Also, the rigid element was used for modeling dies and punches assuming that the dies and punches are rigid bodies in the simulation.

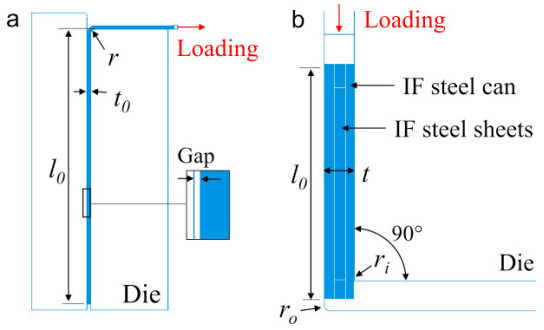

Fig. 9. (a) Open channel drawing; (b) ECAE

The friction coefficient can be an important factor that affects the processes. A sensitivity analysis was conducted based on frictionless and Coulomb friction coefficient of 0.05, 0.08 and 0.1 at the contact interface. It was found that the difference in strains with various coefficient of friction input was very small. Thus, a constant of 0.08, was applied to the interface as the friction between material and die surfaces.

Table 1. Material properties of sheet metal

Material		IF steel	
Density (tones/mm3)		7.85e-9	
Young's modulus (MPa)		210000	
Poisson's ratio		0.3	
True yield stress (σ_p) and plastic strain (ε_p)			
σ_p (MPa)	ε_p (%)	σ_p (MPa)	ε_p (%)
125.60	0.00	281.40	9.80
137.21	0.08	300.00	12.76
163.33	0.82	309.30	14.80
200.00	2.58	323.29	17.00
232.56	4.80	332.50	19.80
250.00	5.97	350.00	24.80
264.83	7.58	358.14	29.80

3.1. Open channel drawing in a 90° die angle

The drawing force and thickness reduction along the length of an open channel drawing were simulated and validated with the experimental results. As shown in Fig. 9(a), the die radius, r, and the sheet metal thickness, t_0, are 0.7mm and the sheet metal length inserted in a die, l_0, is 50 mm. The sheet metal was modeled using the 8630 CPS4R elements and 9504 nodes. The mesh size was 0.07mm. The 0.005 mm gap between the workpiece and the die was applied to decrease the thickness reduction in the process. The workpiece was drawn with the loading velocity of 50.9 mm displacement for 4 seconds.

Fig. 10 shows the deformed shapes of the workpiece from experiment and finite element analysis. Both results present bumps at each end of the front and rear, marked as (A) and (B). The die corner caused the bumps because the sheet had to be vertically pulled out to move. This result also supports the validation of simulation.

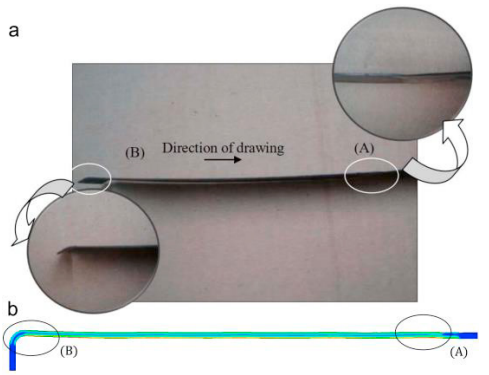

Fig. 10. Deformed shapes (a) Experiment; (b) Simulation model

The thickness along the length from FEA was plotted with the thickness along the length from the experiment. The original thickness of IF steel sheet was 0.7 mm. As shown in Fig. 11, the average thickness from FEA and experiment was approximately 0.65 mm and 0.64 mm, respectively. This

thickness trend with respect to the normalized length supports the validation of simulation. However, uncertain factors such as the frictional effect and contact region may affect the accuracy of FE prediction.

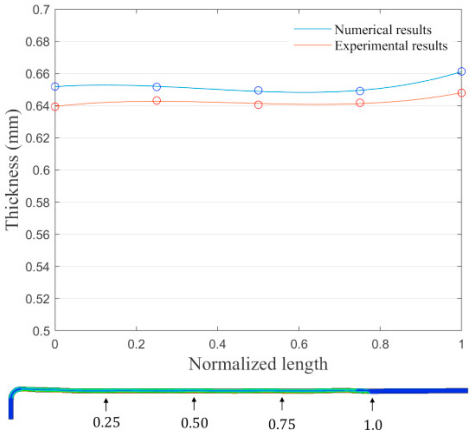

Fig. 11. Comparison of thickness along the length

The drawing force was measured and compared with the numerical results, as shown in Fig. 12. The increasing pattern of the drawing forces was similar up to the peak value. The overall numerical results in steady-state were slightly higher than the experimental results and were oscillating after the peck value. This is because the friction coefficient or the contact region area could vary during the drawing process. In fact, the friction force does not remain as a constant value as the contact area keeps changing during the process.

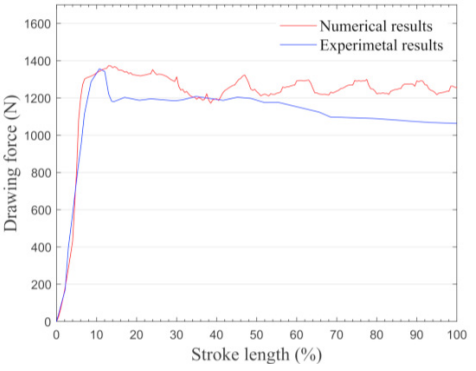

Fig. 12. Comparison of drawing force

The von Mises stress and the equivalent strain were observed to be non-uniform in the contact region between the workpiece and the die as shown in Fig. 13 and Fig. 14. Higher stress was concentrated around the die corner and it gradually decreased as the workpiece is drawn. Also, the strain around the contact region with the die surface was higher compared to other areas. The drawn IF steel workpiece exhibited thickness reduction. On average, the workpiece thickness was decreased by about 6.76 % (see Fig. 11). Thickness reduction of the drawing process is a critical concern for continuous grain refinement of thin metal strips.

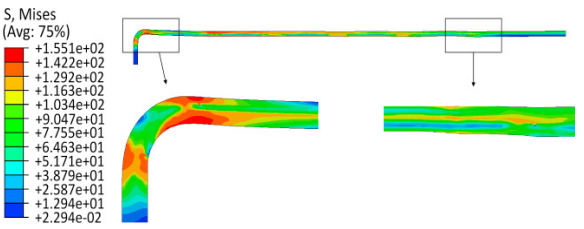

Fig. 13. von Mises stress distribution of open channel drawing

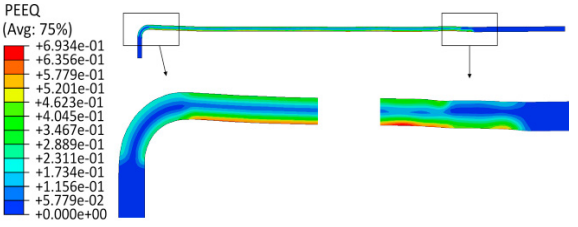

Fig. 14. Equivalent strain distribution of open channel drawing

3.2. Equal channel angular extrusion (ECAE)

The simulation configuration of ECAE was shown in Fig. 9(b). IF steel sheets were pressed in the IF steel can in the experiment and the process was simulated on the assumption that the IF steel can and the sheet metals behave identically and constitute a continuum. Thus, the sheets and the can were modeled in a single domain without having any material or physical boundaries. The ECAE model was meshed using the 5000 CPE4R elements and 5226 nodes. The mesh size was 1 mm. The length of workpiece l_0 = 200 mm, the thickness t = 25.4 mm, the die corner radii r_i = 1 mm and r_0 = 5 mm were set. The channel angle, φ, was 90° and the input loading was 160 mm for 10 seconds.

Fig. 15 and Fig. 16 shows the von Mises stress and equivalent strain distribution in the workpiece after a route 1A process. The shear zone was shown in the corner of the die channel, and the high-stress zone was developed along the cross line between two perpendicular channels in Fig. 15.

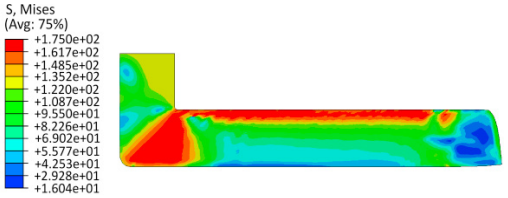

Fig. 15. von Mises stress distribution of ECAE

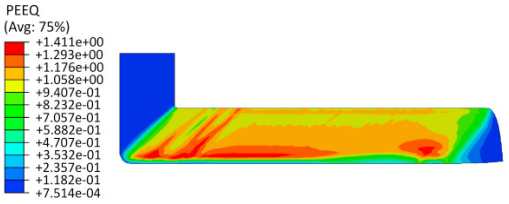

Fig. 16. Equivalent strain distribution of ECAE

In Eq. (3), Iwahashi et al. developed the strain relation by including the curvature angle, ψ, in Segal's strain relation. In the case of the curvature angle of zero, the strain from Eq. (3) is the same as the Eq. (1). The equivalent strain and shear angle in ECAE route 1A were presented and compared in Table 2. Iwahashi's model in Eq. (3) and Eq. (4) was used to consider the curvature angle at the intersection point in the two channels. The equivalent strain and shear angle from FEM were slightly higher than Iwahishi's model in that the friction might affect the shear deformation behavior in the finite element analysis. The FEM results show in good agreement with the theoretical results although a small error remains due to the friction effect or pure shear assumption in Iwahashi's model.

Table 2. Comparison of FEM strain and shear angle

	Equivalent strain	Shear angle (°)
FEM	1.13	63.98
Iwahashi's model	1.09	62.11
Error (%)	3.67	3.01

4. Finite Element Simulation of Combined ECAE and ECAD Processes

There are different continuous processes to achieve UFG materials using billet, wire, or sheet metal. The same concept by Chaudhury et al. [15,17], combining ECAE and ECAD for billet, was used in this work. However, a different possible approach for a continuous process of sheet metal was proposed and the feasibility of the continuous process of the sheet metal was numerically investigated by combining both ECAE and ECAD. Luis [18,19] suggested an ECAE die configuration which has the fillet radius tangent to the die surface, shown in Fig. 17, in contrast to the model of Segal [1] and Iwahashi et al. [5]. It was demonstrated that the configuration has the deformation improvement over the sharp-edged die. In this section, the same radius, 1.0 mm, was used for the inner and outer radius of the die.

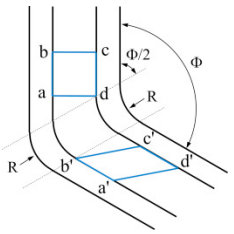

Fig. 17. Schematic of die configuration with the same fillet radius [19]

The assumption was that UFG can be achieved if the process condition can be controlled to generate a stress-strain state that is similar to that of ECAE. FE simulations were conducted to evaluate the feasibility of combining ECAE and ECAD for continuous grain refinement. Different loading conditions were simulated, and the difference was the condition at the entry end with respect to that at the exit end, while the geometry, boundary conditions, and meshes were kept the same. The inputs of the simulation in Fig. 18 were listed in Table 3. Sets of friction rollers pushing the metal sheet is assumed to achieve Loading1, and a pay-off reel provides the condition for Loading2. The simulation model was meshed with the 4230 CPE4R elements and 4484 nodes. The mesh size was 0.2 mm. It was assumed that the die and punches are the rigid bodies that are not to be deformed.

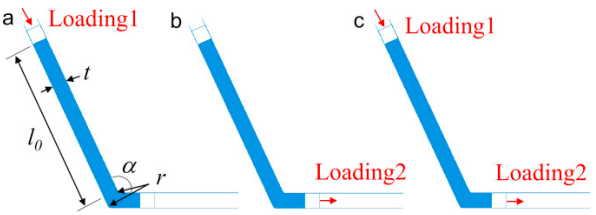

Fig. 18. (a) ECAE; (b) ECAD; (c) Combination of ECAE and ECAD

Table 3. Input parameters for FE simulation

Parameter		Value
Length	l_0	40 mm
Thickness	t	3.5 mm
Radii of a die	r	1.0 mm
Channel angle	α	115°
Friction coefficient	μ	0.08
Input loading	Loading1	35 mm for 3 seconds
	Loading2	35mm for 3 seconds

The same magnitude input loading, approximately the ram speed of 11.67 mm/s, was applied to the entry and/or exit ends in each case. The results of three cases were compared and analyzed to evaluate the possibility of combining ECAE and ECAD. Each max. principal stress distribution and the equivalent strain was provided in Fig. 19 and Fig. 20. All three cases had a similar pattern that the stress was rapidly developed after passing the die corner due to a sharp change of the channel orientation. The stress distribution results of the ECAE and the combined process show that it has an analogous pattern across the thickness. Note that the higher stress of the exit region in Fig. 19(c) compared to the ECAE in Fig. 19(a) was due to the drawing force.

As shown in Fig. 20, the equivalent strain value of three cases evaluated was in the range of 0 to 0.79, and the equivalent strain was not developed before passing the channel crossing. The shapes of strain contour in ECAE and the combined processes were exceedingly similar while the maximum strain value of ECAE was slightly higher than the combined processes. However, the limit of ECAE is that it cannot continuously process the grain refinement for sheet metals while the combined process is advantageous to the continuous

process for sheets. For the ECAD process in Fig. 20(b), inconsistent strain contour was seen and the disadvantage of the ECAD process, the stretching and thinning of the workpiece, was shown in the deformed configuration.

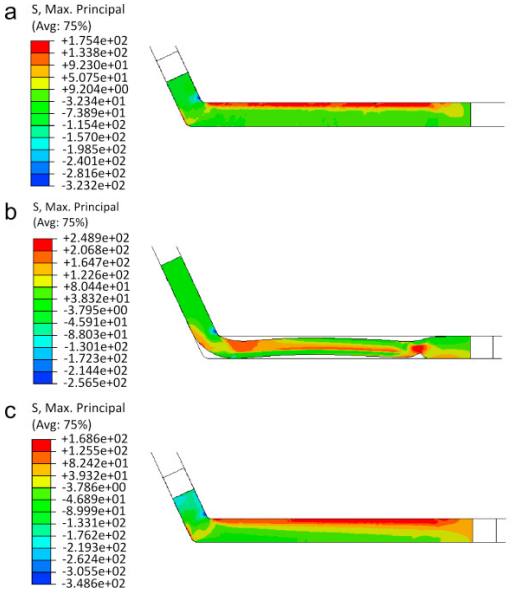

Fig. 19. Max. principal stress distribution (a) ECAE; (b) ECAD; (c) combination of ECAE and ECAD

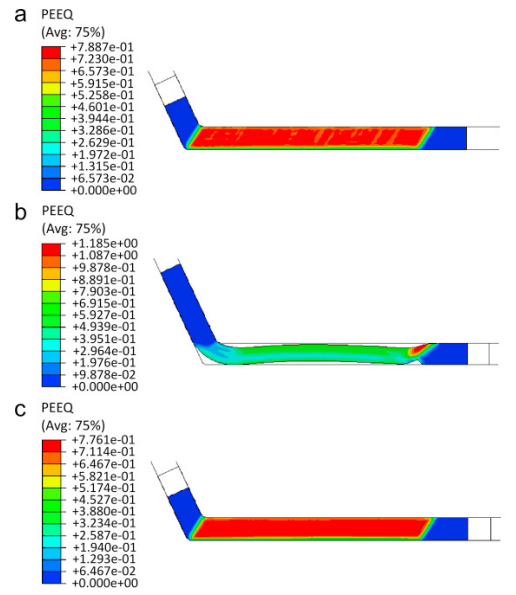

Fig. 20. Equivalent strain distribution (a) ECAE; (b) ECAD; (c) combination of ECAE and ECAD

The thickness reduction of the workpiece was further studied. The origin of the coordinate system is the inside corner of the die. (i.e. $y = 0$ is the upper die and $y = -3.5$ is the lower die.). The thickness along the length was plotted in Fig. 21 and the average thickness was about 2.65 mm while the initial thickness of the IF steel sheets was 3.5 mm. The thickness reduction is one of the main reasons why this process cannot be applied as a continuous process for grain refinement while retaining the initial cross-section [11].

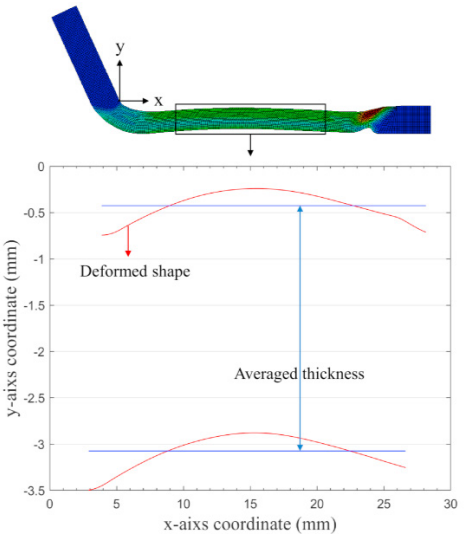

Fig. 21. Thickness reduction of ECAD

The evaluated strain values across the thickness of ECAE, ECAD, and combined ECAE/ECAD were plotted with Iwahashi's strain model in Fig. 22. As shown, ECAE and combined ECAE/ECAD had similar strain distribution, and the strain across the thickness also exhibited a similar pattern. In ECAD, however, the strain across the thickness was non-uniformly developed. The equivalent strain results showed that the ECAD process was not an effective method to obtain uniform strain distribution.

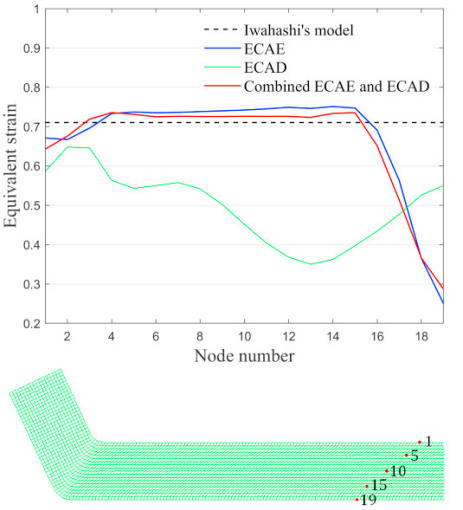

Fig. 22. Comparison of equivalent strain across the thickness

The shear angle across the thickness was plotted in Fig. 23. It can be observed that the shear angle near the contact areas

between the workpiece and the die was less than that of the region in the middle of the cross-section. This effect was caused by the friction of the contact interface. The average values of equivalent strain and shear angle can be slightly higher or lower compared to the theoretical results of Iwahashi's model because numerical results depend on the coefficient of friction input while the friction effect is not considered in Iwahashi's model. The ECAE and combined ECAE/ECAD results showed that the shear angles were distributed around the theoretical value, and the shear angle results imply that the processes can achieve grain refinement.

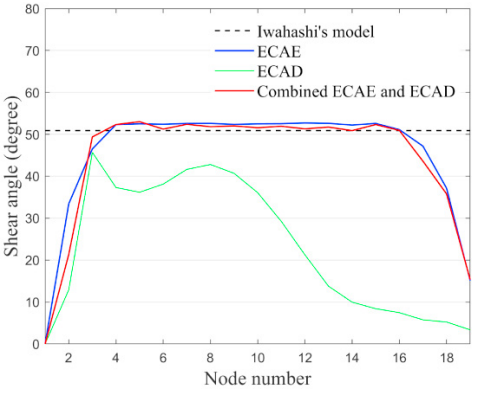

Fig. 23. Comparison of shear angle across the thickness

The shear angles across the thickness of the ECAE and combined ECAE/ECAD summarized in Table 4 were averaged based on the steady-state zone in Fig. 23, while the shear angle of ECAD was calculated based on the whole thickness, node number 1 to 19, due to no die channel contact. The values of the equivalent strain and angle in ECAE and combined ECAE/ECAD had a less than two percent difference from the value of Iwahashi's model. Compared to the ECAE, the ECAD process does not have the desired strain and shear angle. In contrast, the combined ECAE/ECAD process showed noticeable results as the differences in strain and shear angle, compared to that of ECAE, were only 0.14 % and 0.30 %, respectively. The results show that the combination of ECAE and ECAD can facilitate the development of a continuous grain refinement process.

Table 4. Comparison of equivalent strain and shear angle

	Equivalent strain	Shear angle (°)
ECAE	0.72	51.65
ECAD	0.50	22.94
Combined ECAE/ECAD	0.72	51.81
Iwahashi's model of ECAE	0.71	50.89

The thickness reduction along the length from each process was compared as shown in Table 5. The thickness of ECAD was approximately decreased by 24.33 % while the other processes had very little, as low as 0.013 %, thickness reduction. Notice the thickness reduction for the open channel drawing presented earlier was only 6.76 %. This is due to the different sheet thickness to die radius ratios, 1.0 for open channel drawing and 3.5 for ECAD. It is clear that the drawing process causes thickness reduction. The severity of the reduction, however, depends on die geometries (e.g. die angle and radii) and process condition (e.g. friction and feeding and drawing speeds). As such, the weakness of ECAD can be mitigated by adjusting various parameters when combining ECAE and ECAD processes.

Table 5. Comparison of thickness reduction along the length

	Average thickness(mm)	Thickness reduction(mm)
ECAE	3.4995	0.0005
ECAD	2.6481	0.8519
Combined ECAE/ECAD	3.4999	0.0001

5. Conclusions

This paper investigated the feasibility of combining ECAE and ECAD processes for continuous grain refinement of sheet metal. Open channel drawing and pack ECAE were first conducted to evaluate their effects on grain refinement. The stress-strain states of the IF steel workpiece after the process were analyzed using FE simulations. Then, the FE simulations of the possible cases, i.e., a single pass of ECAE, a single pass of ECAD, and combined ECAE/ECAD, were conducted.

Based on the experiment and FEA results, the assumption was that UFG can be achieved if the process condition can be controlled to generate a stress-strain state that is similar to that of ECAE. The main conclusions of the experiments and conceptual studies are as follows:

- The optical microscopy showed that after open channel die drawing, the grain was partially refined at the bottom edge which was the contact surface between die and workpiece. In contrast, the extensive elongated and refined grains were shown after passing 'route 1A' of ECAE. Experiments also showed that, after drawing, the thickness of the strip along the length was significantly reduced.
- The averaged thicknesses of the experiment and FE analysis in the open channel drawing were in good agreement. The drawing force in the steady-state condition calculated from FEA also agreed well with experimental measurement. From simulations, it was further observed that the ECAD and ECAE resulted in workpiece materials with distinct stress-strain states.
- Three different FE simulations based on the same geometry but different loading conditions verified that ECAD, by itself, does not have merits due to thickness reduction and insufficient shear strain. Nevertheless, the thickness reduction of combined ECAD and ECAE was significantly improved and the shear angle was also similar to the shear angle value of ECAE.

Combining ECAE and ECAD for sheet metal can be a viable continuous process in the manufacturing industry. This process can be adjusted to avoid instability such as buckling of the sheet metal generated by the feeding or compressive force to press/extrude. The mechanism of the feeding and pulling system for the continuous process can be explored. The effects

of loading condition on grain refinement can also be further investigated in the future.

Acknowledgements

Finite element analysis using ABAQUS was conducted with the advanced computing resources provided by Texas A&M High Performance Research Computing.

References

[1] Segal VM. Materials processing by simple shear. Materials Science and Engineering: A 1995;197:157–164.
[2] Segal VM. Mechanics of continuous equal-channel angular extrusion. Journal of Materials Processing Technology 2010;210:542–549.
[3] Segal V. modes and processes of severe plastic deformation (SPD). Materials 2018;11:1175.
[4] Segal VM. Slip line solutions, deformation mode and loading history during equal channel angular extrusion. Materials Science and Engineering: A 2003;345:36–46.
[5] Iwahashi Y, Horita Z, Nemoto M, Wang J, Langdon TG. Principle of equal-channel angular pressing for the processing of ultra-fine grained materials. Scripta Materialia 1996;35.
[6] Nakashima K, Horita Z, Nemoto M, Langdon TG. Development of a multi-pass facility for equal-channel angular pressing to high total strains. Materials Science and Engineering: A 2000;281:82–87.
[7] Iwahashi Y, Horita Z, Nemoto M, Langdon TG. The process of grain refinement in equal-channel angular pressing. Acta Materialia 1998;46:3317–3331.
[8] Aour B, Zaïri F, Boulahia R, Naït-Abdelaziz M, Gloaguen J-M, Lefebvre J-M. Experimental and numerical study of ECAE deformation of polyolefins. Computational Materials Science 2009;45:646–652.
[9] Chakkingal U, Suriadi AB, Thomson PF. The development of microstructure and the influence of processing route during equal channel angular drawing of pure aluminum. Materials Science and Engineering: A 1999;266:241–249.
[10] Chakkingal U, Suriadi AB, Thomson PF. Microstructure development during equal channel angular drawing of Al at room temperature. Scripta Materialia 1998;39.
[11] Alkorta J, Rombouts M, De Messemaeker J, Froyen L, Sevillano JG. On the impossibility of multi-pass equal-channel angular drawing. Scripta Materialia 2002;47:13–18.
[12] Zisman AA, Rybin VV, Van Boxel S, Seefeldt M, Verlinden B. Equal channel angular drawing of aluminium sheet. Materials Science and Engineering: A 2006;427:123–129.
[13] Perez CL, Berlanga C, Pérez-Ilzarbe J. Processing of aluminium alloys by equal channel angular drawing at room temperature. Journal of Materials Processing Technology 2003;143:105–111.
[14] Valiev RZ, Islamgaliev RK, Alexandrov IV. Bulk nanostructured materials from severe plastic deformation. Progress in Materials Science 2000;45:103–189.
[15] Chaudhury PK, Srinivasan R, Viswanathan S. Continuous severe plastic deformation process for metallic materials, U.S. Patent No.: US 6,895,79 B15. Date: 24-5-2005 2005.
[16] Naizabekov A, Volokitina I, Volokitin A, Panin E. Structure and Mechanical Properties of Steel in the Process "Pressing–Drawing." Journal of Materials Engineering and Performance 2019;28:1762–71.
[17] Srinivasan R, Chaudhury PK, Cherukuri B, Han Q, Swenson D, Gros P. Continuous severe plastic deformation processing of aluminum alloys. DOE Award Number: DEFC36-01ID14022, Technical Report 2006.
[18] Luri R, Luis CJ, León J, Sebastian MA. A new configuration for equal channel angular extrusion dies. Journal of Manufacturing Science and Engineering 2006;128:860–865.
[19] Pérez CL. On the correct selection of the channel die in ECAP processes. Scripta Materialia 2004;50:387–393.